

Modeling and Analysis of Interference in Listen-Before-Talk Spectrum Access Schemes

Alexe E. Leu¹, Mark McHenry¹, and Brian L. Mark²,

¹Shared Spectrum Company
1595 Spring Hill Road
Vienna, VA 22182

ECE Dept., MS 1G5
George Mason University
Fairfax, VA 22030 Suite 300

Abstract— Spectrum measurement studies have shown that substantial portions of the allocated wireless spectrum are highly underutilized. Frequency agile radios (FARs) have the potential to make opportunistic use of such spectrum holes without causing harmful interference to the users of the allocated spectrum. Toward this goal, we develop a framework for modeling the interference caused by FARs employing spectrum access mechanisms based on the simple Listen-Before-Talk (LBT) scheme. Two variations of LBT are considered: individual LBT, whereby the FARs act independently of each other, and collaborative LBT, whereby the FARs communicate with each other in order to more accurately identify the spectrum holes. Our analysis of the LBT scheme reveals the fundamental interdependencies among key system design metrics and provides a basis for analyzing more complex spectrum access methods. In particular, the analysis of LBT provides a lower bound on the capacity gain achievable by FARs employing spectrum sharing schemes. Our numerical results show that even the individual LBT scheme can provide capacity gains, while even more gain can be achieved using the collaborative LBT schemes. Our analysis suggests that much greater gains should be achievable via spectrum access schemes that incorporate location information and/or more sophisticated group behaviors.

I. INTRODUCTION

In conventional wireless systems, the wireless spectrum is statically allocated among various transmitters located over a geographic coverage area. Recent studies of wireless spectrum usage [1], [2] suggest that significant portions of the wireless spectrum are highly underutilized. An open research question is whether such “spectrum holes” can be exploited without causing harmful interference to the primary users, i.e., transmitters and receivers, of the allocated wireless spectrum. In this paper, we model the interference caused to the primary users by frequency agile radios (FARs), which attempt to identify and make use of the spectrum holes by using an access mechanism called Listen-Before-Talk (LBT).

Frequency agile radios [1], also known as spectrum agile radios, have the ability to transmit and receive signals on dynamically tunable frequency ranges. Spectrum agility is a key property of the next generation of cognitive radios [3], [4]. If a group of FARs could detect the presence of a spectrum hole in a given frequency range, the group would be able to communicate on frequency channels lying within the hole. In this scenario, the FARs must transmit with sufficient power to communicate with each other, but

must not cause harmful interference to the primary users. Identification of spectrum holes is made possible by highly sensitive detectors [5]

The FARs may collaborate with each other to identify the spectrum holes. In general, the FAR nodes do not communicate with the primary users. For this reason, the primary nodes are sometimes referred to as *non-cooperative* nodes. The non-cooperative nodes may be divided into transmitters and receivers. We refer to the transmitters as primary transmitters and the receivers as *victim* nodes, to emphasize that the FARs may cause some interference to these receivers. A spectrum sharing access scheme must ensure that such interference is maintained below a certain tolerable threshold.

The main objective of this paper is to model the interference to the victim nodes caused by a group of FAR nodes employing two variations of the LBT scheme: individual LBT and collaborative LBT. In the individual LBT scheme, each FAR node listens to a given frequency channel for a short time interval called the *listen period* before attempting to transmit on the channel. If the received signal measurement at the FAR node exceeds a certain threshold, called the *detection threshold*, the FAR node abandons the current frequency channel and moves on to a different channel. Otherwise, the FAR node transmits on the channel for a short time interval called the *transmit period*. In the collaborative LBT scheme, if at least one FAR node in a group detects the presence of a signal in a given frequency channel during its listen period, all FAR nodes in the group are alerted to refrain from transmitting on the channel. Collaborative LBT requires the exchange of special alert messages among the FAR nodes. Other variations of LBT are possible, but modeling the interference caused by these simple LBT schemes provides a basis for studying more sophisticated spectrum access schemes (cf. [6]).

Most of the previous research on resource management for wireless networks has focused on systems in which all of the nodes may cooperate with one another, typically in an infrastructured environment (cf. [7]). By contrast, the scenario considered in this paper divides consists of two subsystems: a non-cooperative system consisting of the set of primary users and a cooperative system consisting of the set of FAR nodes. **The goal of the FAR nodes is to make use of the wireless spectrum that is unused**

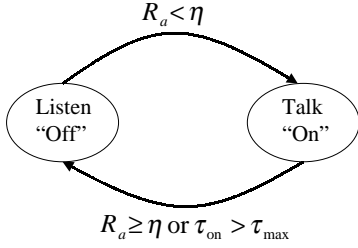


Fig. 1. State transition diagram of individual LBT.

by the primary users without causing harmful interference. Thus, an analysis of the interference to the victim nodes caused by the FAR nodes employing a spectrum access scheme such as LBT is an important step in developing effective spectrum sharing technologies.

The remainder of the paper is organized as follows. Section II describes the LBT schemes in further detail. Section III describes the basic model of interference between the FAR nodes employing LBT and the primary users. Analytical expressions for the probability of interference for individual LBT are derived in section IV. Section V extends this analysis to the collaborative LBT scheme. Section VI presents numerical results showing the performance of the two types of LBT schemes under a wide range of parameter settings. Finally, the paper is concluded in section VII.

II. LISTEN-BEFORE-TALK SPECTRUM ACCESS

A. Overview of Spectrum Access Methods

Spectrum methods can loosely be classified as cooperative or noncooperative [6].

B. Individual LBT

The Listen-Before-Talk (LBT) algorithm is a simple scheme for an FAR node to access a radio frequency channel opportunistically. Consider a radio frequency channel c centered at the carrier frequency f_c and spanning the range $[f_c - \Delta_f, f_c + \Delta_f]$. Thus, the bandwidth of the channel is given by $B_c = 2\Delta_f$. The LBT scheme consists of two states: 1) *listen* or *off* state and 2) the *talk* or *on* state. During the listen state, FAR node does not transmit a signal and estimates the received signal power R in the radio channel c , given by

$$R = \int_{f_c - \Delta}^{f_c + \Delta} G_R(f) df, \quad (1)$$

where $G_R(f)$ is an estimate of the (one-sided) power spectral density of the received signal.

In the *off* state, the FAR node also estimates a transmit power level, s^* , which we refer to as the *maximum interference-free transmit power* (MIFTP). The MIFTP is defined as the maximum power at which the FAR node can transmit without causing harmful interference to any of the victim nodes. If the received signal power R from the primary transmitter falls below a value η called the *detection threshold*, the FAR node transitions to the *on* state.

Otherwise, the FAR node remains in the off state either for the same channel c or a different frequency channel c' . For simplicity, our analysis shall only consider the case where the FAR node stays in the same channel c . During the on state, the FAR node transmits at the MIFTP power level s^* for a maximum duration τ_{max} , and then returns to the off state. During the off state, the FAR node continues to listen to the channel and returns to the off state if $R < \eta$. Fig. 1 illustrates the LBT algorithm by means of a state transition diagram.

In this paper, we shall ignore the channel contention among FAR nodes accessing the same channel. Such contention can be resolved using a suitable medium access control (MAC) protocol. Thus, the maximum transmission duty cycle of an FAR node on a given channel is given by

$$d_{max} = \frac{\tau_{on}}{\tau_{on} + \tau_{off}}, \quad (2)$$

where τ_{off} is the average duration in the off state. Clearly, the amount of interference caused to the victim nodes by an FAR node performing LBT depends on the values of the key parameters η , τ_{on} , and the MIFTP s^* . The interdependencies among these parameters are analyzed in section IV.

C. Collaborative LBT

Collaborative LBT extends the individual LBT scheme by allowing a group of FAR nodes to share information gathered during the listen period with each other via alert messages. In collaborative LBT, each FAR node in the group executes the individual LBT algorithm for a given frequency channel c as discussed earlier with the following modification. If at least one FAR node in the group detects the presence of a signal from a primary transmitter, then all of the FAR nodes in the group turn off and revert to the listen state. Otherwise, the channel c is then accessed by the group of FAR nodes using a medium access control (MAC) protocol. Again, we shall not concern ourselves with the details of the MAC protocol used among the FAR nodes. We shall simply choose a particular FAR node in the group and assume that it can transmit at MIFTP during its talk period without causing interference to the other FAR nodes.

III. INTERFERENCE MODEL

In this section, we develop a simple model to characterize the interference caused by an FAR node to a victim receiver.

A. Interference scenario

Consider a scenario consisting of a three nodes: a primary transmitter p , a victim receiver v , and a frequency agile node denoted by a , as shown in Fig. 2. The transmitter p transmits on frequency channel c , while node a performs LBT on the channel. The receiver v , expects to receive the transmissions of node p . However, node a may cause interference to node v during the talk state of LBT.

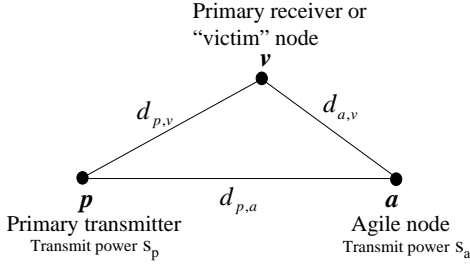


Fig. 2. Interference scenario.

Denote the geographic locations of the nodes by (x_i, y_i) , where $i \in \{a, p, v\}$. Let d_{ij} and L_{ij} denote, respectively the distance and propagation loss from node i to node j , where $i, j \in \{a, p, v\}$. Clearly, the propagation loss L_{ij} depends on the propagation distance d_{ij} . We model the primary transmitter p and the FAR node a as on-off sources. In the off-states, both sources do not transmit signals. In the on-states, node p transmits with power s_p , while node a transmits with power s_a in the off-state. The received signal power from the primary transmitter p during its on-state at nodes a and v can be expressed as follows:

$$R_a = s_p - L_{p,a}, \quad (3)$$

$$R_v = s_p - L_{p,v}. \quad (4)$$

Similarly, we represent the interference signal power from node a received at node v is given by

$$I_v = s_a - L_{a,v} \quad (5)$$

Mathematically, all of the quantities in (3)-(5) are stochastic processes, although the time parameter t has been suppressed in the above equations to emphasize the steady-state condition.

For successful reception of the primary signals from node p at node v , certain conditions must be satisfied. Let r_{min} denote the minimum received signal level required by the primary receiver v from the primary transmitter p . Denote by i_{max} the maximum allowable interference that node v can tolerate. Let $E_a^{(on)}$ and $E_p^{(on)}$ denote, respectively, the events that nodes a and node p are in the on state. Then the event that node a causes harmful interference to node v , i.e., the *interference event* can be expressed as follows:

$$E_{int} = \{R_v \geq r_{min}, E_p^{(on)}\} \cap \{I_v \geq i_{max}, E_a^{(on)}\}. \quad (6)$$

Thus, the interference event occurs if and only if the primary transmitter p is on and the received signal at node v from p exceeds r_{min} and node a is on and the received interference signal at node v from a exceeds i_{max} .

B. Propagation model

The signal propagation loss is modeled as a sum of three components: path loss, lognormal shadowing noise, and Rayleigh fast fading. We shall assume that the fast fading

can be eliminated by averaging the received signal measurements over time. Thus, the propagation loss between nodes i and j can be expressed as

$$L_{ij} = D_{ij} + W_{ij}, \quad (7)$$

where D_{ij} and W_{ij} represent the path loss and shadowing noise, respectively. In general, the path loss is a function several variables:

- the locations of nodes i and j and the nature of the geographic terrain between them;
- the transmitter antenna height $h_i^{(t)}$;
- the receiver antenna height $h_j^{(r)}$;
- the carrier frequency f_c ;
- the antenna polarization o_i (horizontal or vertical).

The shadowing component W_{ij} is assumed to be zero-mean white Gaussian noise process with variance σ_{ij}^2 and independent of the path loss D_{ij} .

The path loss D_{ij} component can be modeled using the empirical propagation model (EPM-73) [10] or more complicated propagation prediction models such as the Longley-Rice model [11], [12] or the TIREM (Terrain Integrated Rough Earth Model) [13]. For simplicity, we shall assume the EPM-73 model in this paper. According to the EPM-73 model, the mean path loss for a given terrain type (hilly, swamp, etc.) depends only on the distance between the two nodes. Hence, we can write

$$D_{ij} = g(d_{ij}, h_i^{(t)}, h_j^{(r)}, f_c, o_i), \quad (8)$$

where the function $g(\cdot)$ is given in [10]. For notational convenience, we shall simply write $D_{ij} = g(d_{ij})$ and suppress the dependence of the path loss on the remaining four parameters. Since the function $g(\cdot)$ is invertible, the distance can be expressed in terms of the path loss by

$$d_{ij} = g^{-1}(D_{ij}). \quad (9)$$

IV. ANALYSIS OF INDIVIDUAL LBT

In this section, we derive expressions for the interference probability for the individual LBT scheme based on the interference model discussed in section III. We also derive several other key system parameters and discuss their performance impacts.

A. Outage probability and coverage distance

The *outage probability* (of node v) is defined by

$$P_{out} \triangleq P\{R_v < r_{min} | E_p^{(on)}\}. \quad (10)$$

Hence,

$$P\{R_v \geq r_{min} | E_p^{(on)}\} = (1 - P_{out}). \quad (11)$$

Assuming the EPM-73 propagation path loss model, from (4), (7), and (8), we can write

$$R_v = s_p - g(d_{p,v}) + W_{p,v}. \quad (12)$$

Therefore,

$$P_{out} = 1 - Q\left(\frac{r_{min} + g(d_{p,v}) - s_p}{\sigma_{p,v}}\right). \quad (13)$$

Closely related to the outage probability is the *coverage distance*, d_{cov} , defined as the maximum distance between the primary transmitter and the victim node such that the outage probability does not exceed a value ϵ_{out} :

$$d_{cov}(\epsilon_{out}) \triangleq \max\{d_{p,v} : P_{out} \leq \epsilon_{out}\}. \quad (14)$$

From (13) and (12), we can write

$$d_{cov} = g^{-1}(s_p - r_{min} + \sigma_{p,v}Q^{-1}(1 - \epsilon_{out})). \quad (15)$$

We define the *detection probability*, P_{det} , at the FAR node as the probability that the received signal from the primary transmitter is greater than or equal to a given threshold η . That is, P_{det} is given by

$$P_{det} = P\{R_a \geq \eta\} = 1 - Q\left(\frac{s_p - g(d_{p,a}) - \eta}{\sigma_{p,v}}\right). \quad (16)$$

The *detection distance*, d_{det} at the FAR node is defined as the maximum distance between the FAR node and the primary transmitter such that the probability of detection at the FAR node exceeds a value ϵ_{det} :

$$d_{det}(\epsilon_{det}) \triangleq \max\{d_{a,p} : P_{det} \geq \epsilon_{det}\} \quad (17)$$

Assuming that the function $g^{-1}(\cdot)$ is smooth, from (16) and (17), we have

$$d_{det}(\epsilon_{det}) = g^{-1}(s_p - \eta - \sigma_{p,v}Q^{-1}(1 - \epsilon_{det})), \quad (18)$$

The detection distance decreases monotonically with the bound on the detection probability, ϵ_{out} , which we will show numerically in section VI.

B. Interference probability and distance

The signal power received by node v from node p in the on-state is independent of the interference power it receives from node a in the on-state. Therefore, from (6) we have

$$P_{int} = P\{R_v \geq r_{min}, E_p^{(on)}\} \cdot P\{I_v \leq i_{max}, E_a^{(on)}\}. \quad (19)$$

From (5), (7), and (8), we can write

$$I_v = s_a - g(d_{a,v}) + W_{a,v}. \quad (20)$$

Therefore,

$$P\{I_v \leq i_{max} | E_a^{(on)}\} = Q\left(\frac{i_{max} + g(d_{a,v}) - s_a}{\sigma_{a,v}}\right), \quad (21)$$

where $Q(x) \triangleq \frac{1}{\sqrt{2\pi}} \int_x^\infty e^{-t^2/2} dt$ is the standard Q-function. Using (19), (11), and (21), we obtain the following expression for the interference probability:

$$P_{int} = (1 - P_{out}) \cdot P(E_p^{(on)})P(E_a^{(on)}) \cdot Q\left(\frac{i_{max} + g(d_{a,v}) - s_a}{\sigma_{a,v}}\right). \quad (22)$$

From (22), we can obtain an expression for the transmit signal power of the FAR node in terms of the interference and outage probabilities as follows:

$$s_a = \sigma_{a,v}Q^{-1}\left(1 - \frac{P_{int}}{(1 - P_{out})P(E_p^{(on)})P(E_a^{(on)})}\right) + i_{max} + g(d_{a,v}). \quad (23)$$

To proceed further with the interference analysis of LBT, we make the following worst-case assumptions about the on-off source behavior of the primary transmitter and the FAR node:

- The primary transmitter is always in the on state, i.e., $P(E_p^{(on)}) = 1$.
- The FAR node is in the on state if and only if the received signal from the primary transmitter falls below the threshold η .

With reference the LBT state diagram of Fig. 1, the second assumption is tantamount to the assumption that $\tau_{max} = \infty$. In this case, we have that

$$P(E_a^{(on)}) = 1 - P_{det}.$$

Under the above two assumptions, the duty cycle of the FAR node executing LBT is given by (cf. (2))

$$d_a = P(E_a^{(on)}) = 1 - P_{det}.$$

Let ϵ_{int} be the maximum interference probability that can be tolerated by the victim node v . Under these assumptions, we define the *interference distance*, $d_{int}(\epsilon_{int})$, as the minimum permissible distance between the FAR node a and the victim node v such that the interference probability does not exceed ϵ_{int} .

$$d_{int}(\epsilon_{int}) \triangleq \min\{d_{a,v} : P_{int} \leq \epsilon_{int}\}. \quad (24)$$

From (22), we obtain the following expression for the interference distance:

$$d_{int} = g^{-1}\left(s_a - i_{max} - \sigma_{a,v}Q^{-1}\left(1 - \frac{\epsilon_{int}}{(1 - P_{out})(1 - P_{det})}\right)\right). \quad (25)$$

C. Avoidance of harmful interference

The victim node is said to suffer *harmful interference* from the FAR node under the following conditions:

$$P_{out} \leq \epsilon_{out}, \quad P_{det} \leq \epsilon_{det}, \quad P_{int} > \epsilon_{int}. \quad (26)$$

The first condition states that the outage probability of the victim node should not exceed the threshold ϵ_{out} . If the outage probability exceeds ϵ_{out} , the victim node is oblivious to interference from the FAR node. The second condition requires the detection probability not to exceed the detection probability threshold ϵ_{det} , which implies that the duty cycle of the FAR node would be at least $1 - \epsilon_{det}$. Finally, the third condition requires the probability of interference to be greater than a threshold ϵ_{int} .

From (22), we can derive an expression for the maximum power at which the FAR node can transmit while avoiding harmful interference to node v for a given inter-nodal distance $d_{a,v}$:

$$s_a^* = i_{max} + g(d_{a,v}) + \sigma_{a,v} Q^{-1} \left(1 - \frac{\epsilon_{int}}{(1 - P_{out})(1 - P_{det})} \right). \quad (27)$$

We call s_a^* the *maximum interference-free transmit power* (MIFTP). The MIFTP plays a key role in LBT-based spectrum access.

Assume that the transmit powers of the FAR node and the primary transmitter are fixed at s_a and s_p , respectively. The following proposition gives a simple sufficient condition for the victim node *not* to suffer harmful interference in terms of an inequality relating the coverage distance, the detection distance, and the interference distance.

Proposition 1: Suppose that the first two conditions in (26) hold, i.e.,

$$P_{out} \leq \epsilon_{out} \text{ and } P_{det} \leq \epsilon_{det}. \quad (28)$$

Then the victim node does not suffer harmful interference if

$$d_{int} \leq d_{det} - d_{cov} \quad (29)$$

Proof: By definition, the conditions $P_{out} \leq \epsilon_{out}$ and $P_{det} \leq \alpha$ imply

$$d_{p,v} \leq d_{cov} \text{ and } d_{a,p} \geq d_{det}, \quad (30)$$

respectively. Using the triangle inequality, we have

$$d_{a,v} \geq d_{a,p} - d_{p,v}. \quad (31)$$

From (30) and (31), we have

$$d_{a,v} \geq d_{det} - d_{cov} \geq d_{int}, \quad (32)$$

which implies that

$$P_{int} \leq \epsilon_{int}. \quad (33)$$

Hence, the harmful interference condition (26) does not hold. ■

Clearly, the converse of Proposition (1) does not hold in general. The FAR node can always be positioned sufficiently far from the victim and primary nodes in order to avoid harmful interference. A graphical illustration of Proposition 1 is given in Fig. 3. In Fig. 3, we have that both victim nodes v_1 and v_2 are within a distance d_{cov} from the primary transmitter. Hence, the outage probabilities of the victim nodes do not exceed ϵ_{out} . The FAR node a lies just outside the distance d_{det} from the primary transmitter. Hence, the detection probability does not exceed ϵ_{det} .

Observe that although node v_1 lies beyond the detection distance, d_{det} , from the agile node a , the node v_2 does

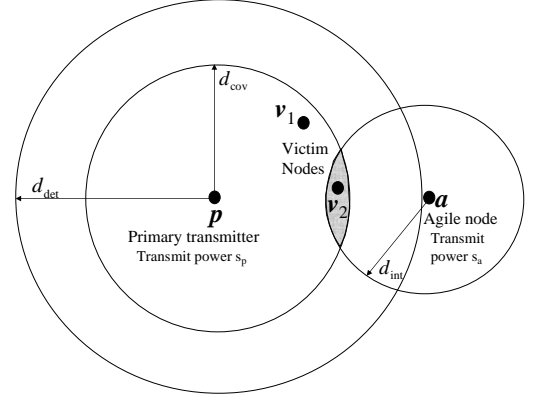


Fig. 3. Interference condition.

not. Hence, node v_2 suffers from harmful interference, i.e., the interference probability experienced by node v_2 exceeds ϵ_{int} . Moreover, any victim node lying within the shaded region would suffer harmful interference. The shaded region can be reduced by lowering the transmit power, s_a . The absence of the shaded region corresponds to the noninterference condition (29). If this condition holds, no victim node can suffer harmful interference from the FAR node.

V. ANALYSIS OF COLLABORATIVE LBT

In collaborative LBT, we consider a group of n FAR nodes $\mathcal{G} = \{a_1, \dots, a_n\}$. Each of these nodes executes the individual LBT algorithm with the proviso that if at least one node in the group detects a signal from the primary transmitter, all nodes in the group turn to the off state. Otherwise, each node is in the on state transmitting at a certain power level. Let R_{a_i} denote the signal power from the primary transmitter that is received at FAR node a_i (cf. (3)):

$$R_{a_i} = s_p + L_{p,a_i}. \quad (34)$$

Then the probability that the FAR nodes are all in the on state is given by

$$P(E_a^{(on)}) = P \left[\bigcap_{i=1}^n \{R_{a_i} < \eta\} \right], \quad (35)$$

where η is the detection threshold. Assuming that the received signal strengths are independent,

$$\begin{aligned} P(E_a^{(on)}) &= \prod_{i=1}^n P\{R_{a_i} < \eta\} \\ &= \prod_{i=1}^n Q \left[\frac{s_p - \eta - g(d_{p,a_i})}{\sigma_{p,a_i}} \right]. \end{aligned} \quad (36)$$

Let α be the probability that all the FAR nodes are in the off state, i.e.,

$$\begin{aligned} \alpha &= 1 - P(E_a^{(on)}) \\ &= 1 - \prod_{i=1}^n Q \left[\frac{s_p - \eta - g(d_{p,a_i})}{\sigma_{p,a_i}} \right]. \end{aligned} \quad (37)$$

If all nodes in \mathcal{G} are equidistant from node p and the propagation characteristics from p to the FAR nodes are *homogeneous*, then

$$\alpha = 1 - Q^n \left(\frac{s_p - \eta - g(d_{p,a})}{\sigma_{p,a}} \right), \quad (38)$$

where $d_{p,a}$ is the common distance from node p to each FAR node, and $\sigma_{p,a}$ is the common shadowing standard deviation. Under the assumption of homogeneity of the FAR nodes with respect to node p , we can define a detection distance analogous to (18), with α given by (38). Similarly, we can define an interference distance analogous to (25) and an MIFTP analogous to (27).

VI. NUMERICAL RESULTS

In this section, **we present numerical results showing performance metrics for individual and collaborative LBT over a range of parameter values** using the expressions derived in sections IV and V. The results provide insight into the performance impacts of the various key system parameters in LBT spectrum access.

A. Interference, coverage, and detection distances

Figs. 4 and 5 show plots of the detection distance d_{det} as a function of the maximum detection probability ϵ_{det} for different values of the detection threshold η in individual LBT. Fig. 4 shows curves obtained for a carrier frequency of $f_c = 200$ MHz, while Fig. 5 corresponds to $f_c = 2.4$ GHz. The frequency $f_c = 200$ MHz lies within the transmission band of television towers, while $f_c = 2.4$ GHz lies within the transmission band of MMDS (Multipoint Microwave Distribution System) systems. The detection distance curves were obtained using (18). The graphs also show the sum of the interference and coverage distances, i.e., $d_{int} + d_{cov}$, as a function of the detection probability ϵ_{det} . The values of d_{int} and d_{cov} were calculated using (25) and (15), respectively. The other system parameters of interest are set as follows:

- FAR transmitter power $s_a = 40$ dBm,
- FAR and victim node receiver antenna heights

$$h_a^{(r)} = h_v^{(r)} = 3 \text{ m},$$

- FAR and primary transmitter antenna heights

$$h_a^{(t)} = h_p^{(t)} = 10 \text{ m},$$

- Primary transmitter power $s_p = 80$ dBm,
- Interference probability $P_{int} = 0.01$,
- Maximum outage probability $P_{out} = 0.1$.

The detection threshold ranges from $\eta = -136$ dBm to $\eta = -106$ dBm.

Observe that both the detection distance and the interference distance are monotonically decreasing functions of the detection probability. To avoid harmful interference, the detection threshold η should be chosen such that the non-interference condition (29) holds over the entire range

of values of ϵ_{int} , since we have no prior knowledge of the detection probability. With respect to Figs. 4 and 5, the non-interference condition requires the d_{det} curve to lie above the $(d_{int} + d_{cov})$ curve for all values of α .

We observe that the non-interference condition holds when the detection threshold satisfies $\eta = -136$ dB for both carrier frequencies. This implies a lower bound on the sensitivity of the detector of the FAR node to ensure that it does not cause harmful interference to the victim node. Note that at the higher carrier frequency $f_c = 2.4$ GHz, the interference, detection, and coverage curves are all significantly lower than at $f_c = 200$ MHz. When $f_c = 2.4$ GHz, the peak value of $d_{int} + d_{cov}$ is about 175 km, whereas the corresponding value at $f_c = 200$ MHz is about 460 km.

B. MIFTP vs. Detection Threshold

Fig. 6 show curves of the MIFTP as a function of the detection threshold η for the carrier frequencies $f_c = 200$ MHz and $f_c = 2.4$ GHz, respectively. Observe that the MIFTP curve for $f_c = 2$ GHz lies below the curve for $f_c = 200$ MHz. Thus, at lower carrier frequencies the FAR node can transmit with higher signal power without causing harmful interference to the victim receiver.

C. MIFTP vs. interference probability

Figs. 7 and 8 show surfaces of the MIFTP as a function of the detection threshold η and the interference probability P_{int} for the carrier frequencies $f_c = 200$ MHz and $f_c = 2.4$ GHz, respectively. We observe that the surface corresponding to $f_c = 2$ GHz lies below the surface for $f_c = 200$ MHz. The decreasing trend of the MIFTP with respect to the detection threshold is similar at both carrier frequencies.

D. MIFTP vs. FAR transmitter antenna height

Figs. 9 and 10 show surfaces of the MIFTP as a function of the detection threshold η and the FAR transmitter antenna height $h_a^{(t)}$ for $f_c = 200$ MHz and $f_c = 2$ GHz, respectively. At both carrier frequencies, the MIFTP increases linearly with increasing antenna height. Note that the MIFTP surface at the higher carrier frequency has a larger slope with respect to the FAR transmitter antenna height compared to the MIFTP surface at the lower frequency. In fact, the two surfaces, cross each other at an antenna height of approximately 150 m.

E. MIFTP vs. carrier frequency

Fig. 11 shows an MIFTP surface as a function of the detection threshold η and the carrier frequency f_c . The MIFTP surface is a decreasing function of η , but is not a monotonic function of f_c . As can be observed in Fig. 11, the MIFTP decreases roughly linearly as f_c is increased from 0 Hz to about 500 MHz. Then the MIFTP increases linearly as f_c increases from 500 MHz to a maximum value of 65 MHz when f_c is approximately 1200 Hz. Finally, the MIFTP decreases linearly for f_c larger than 1200 Hz.

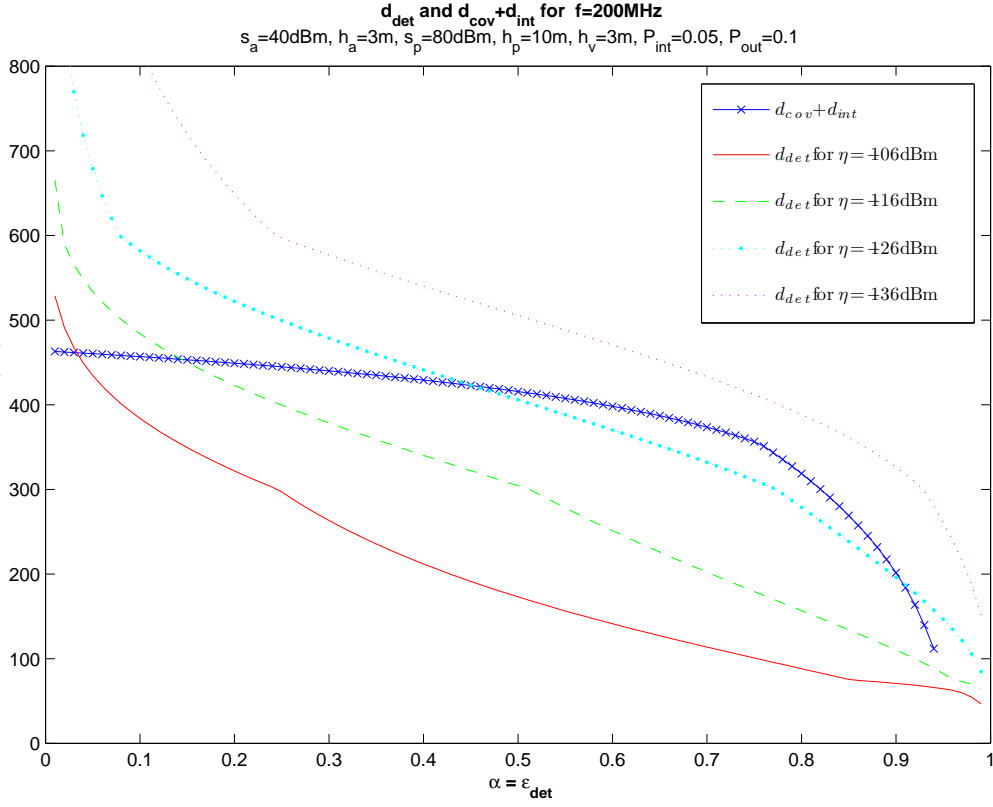


Fig. 4. Interference, coverage, and detection distances for $f_c = 200$ MHz.

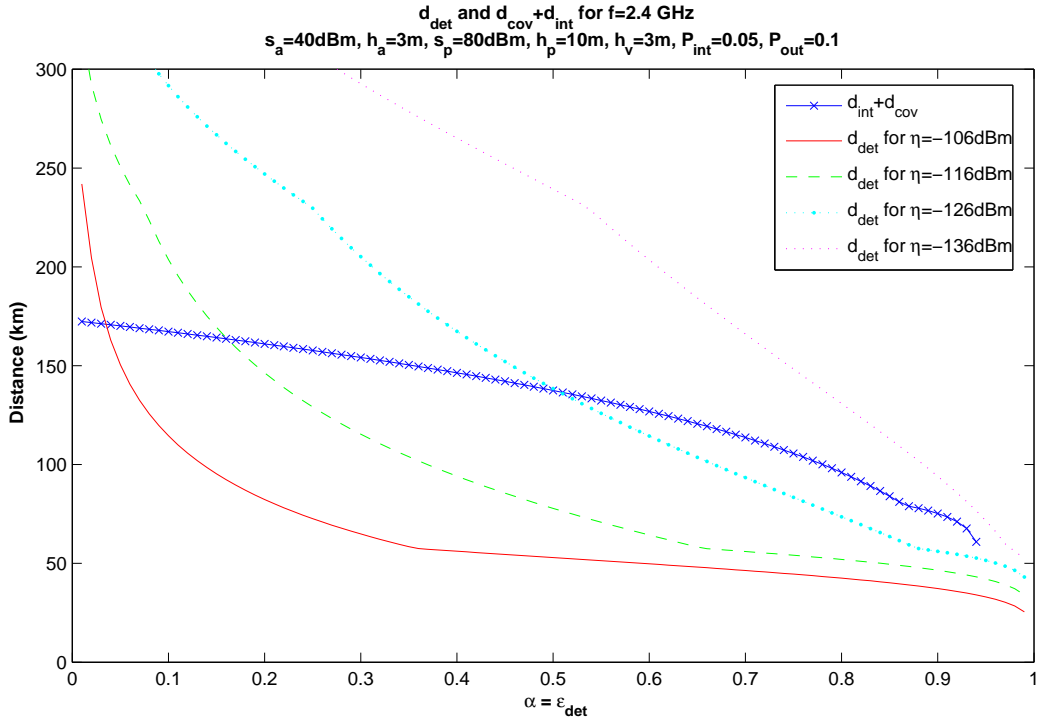


Fig. 5. Interference, coverage, and detection distances for $f_c = 2.4$ GHz.

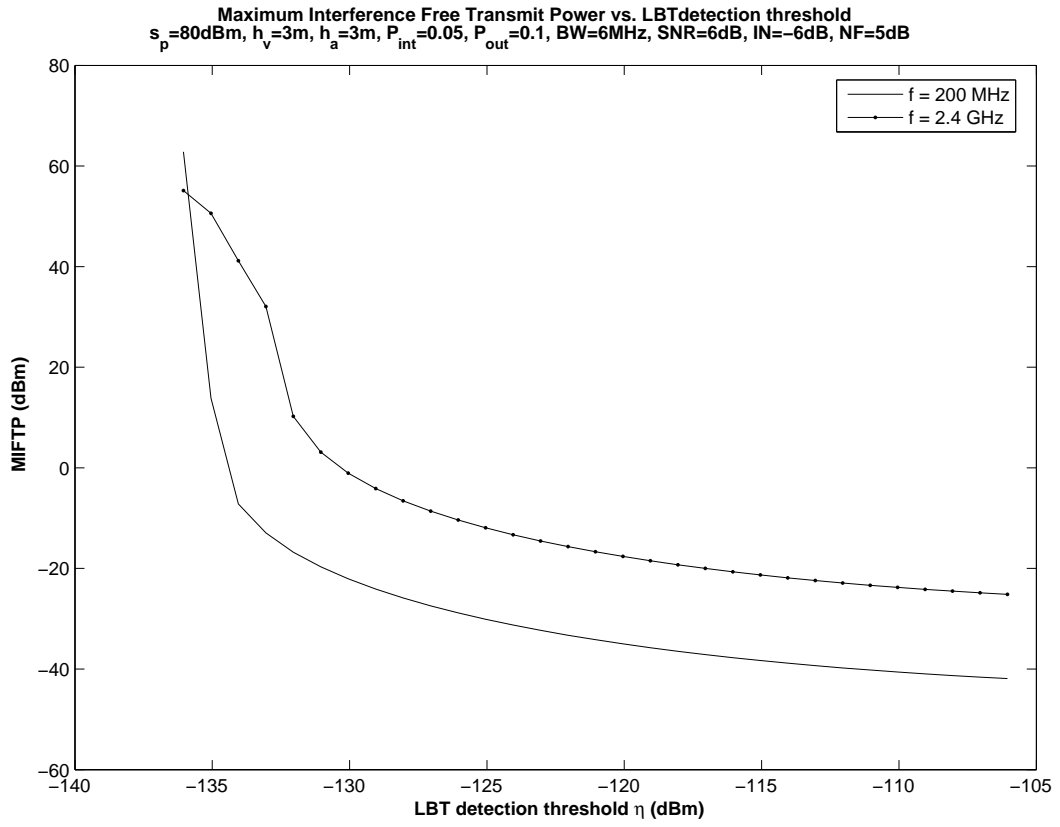


Fig. 6. MIFTP vs. LBT detection threshold η .

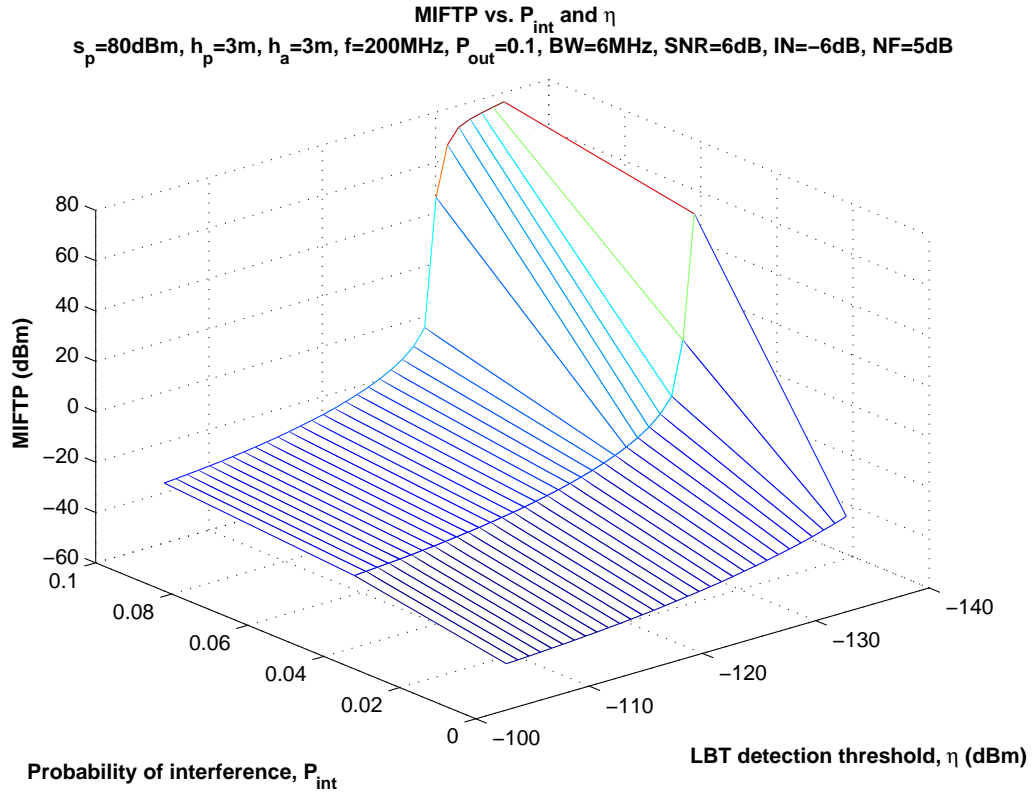


Fig. 7. MIFTP vs. detection threshold and interference probability for $f_c = 200$ MHz.

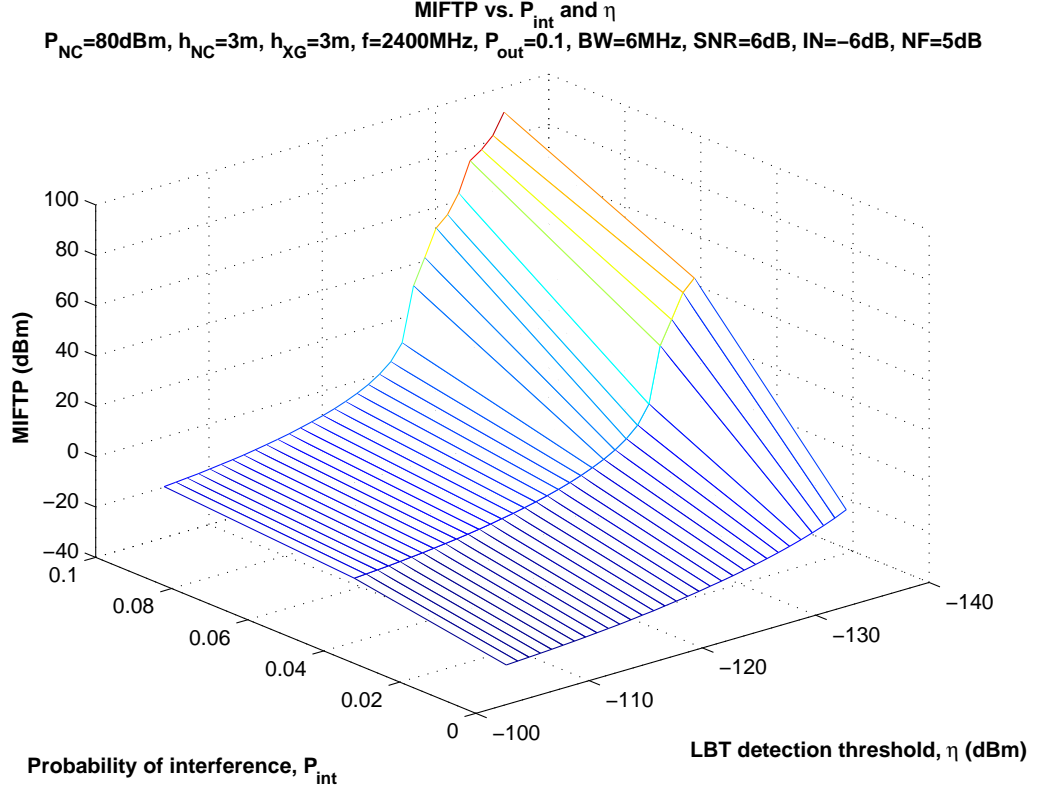


Fig. 8. MIFTP vs. detection threshold and interference probability for $f_c = 2.4$ GHz.

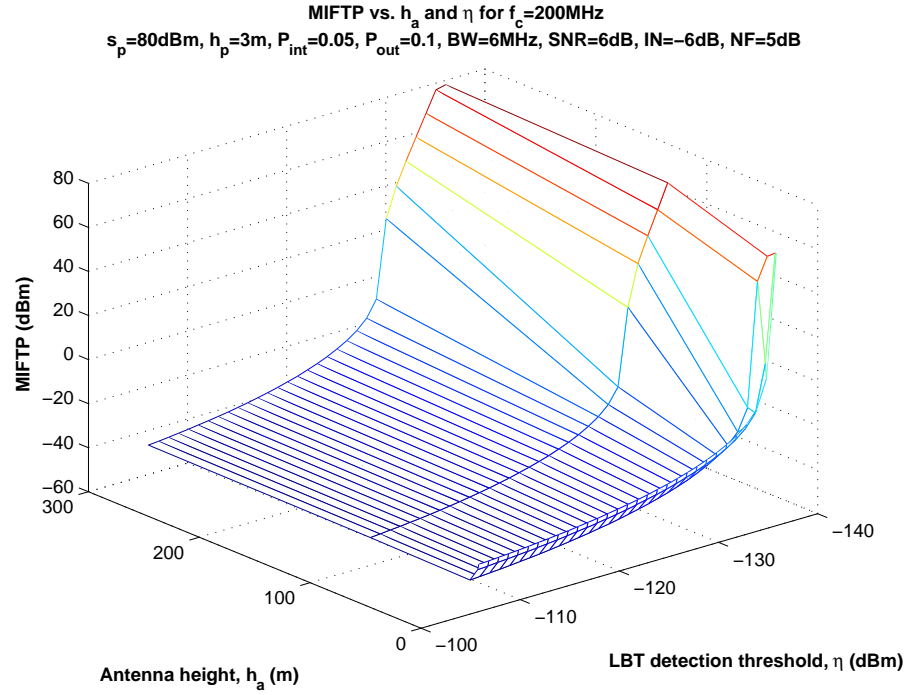


Fig. 9. MIFTP vs. detection threshold and FAR transmitter antenna height for $f_c = 200$ MHz.

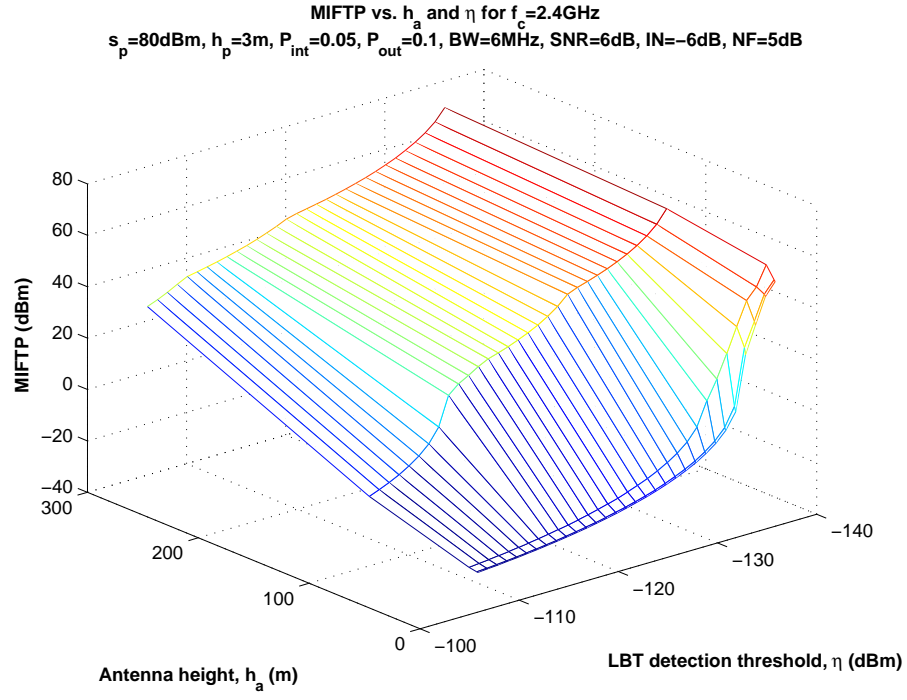


Fig. 10. MIFTP vs. detection threshold and FAR transmitter antenna height for $f_c = 2.4\text{ GHz}$.

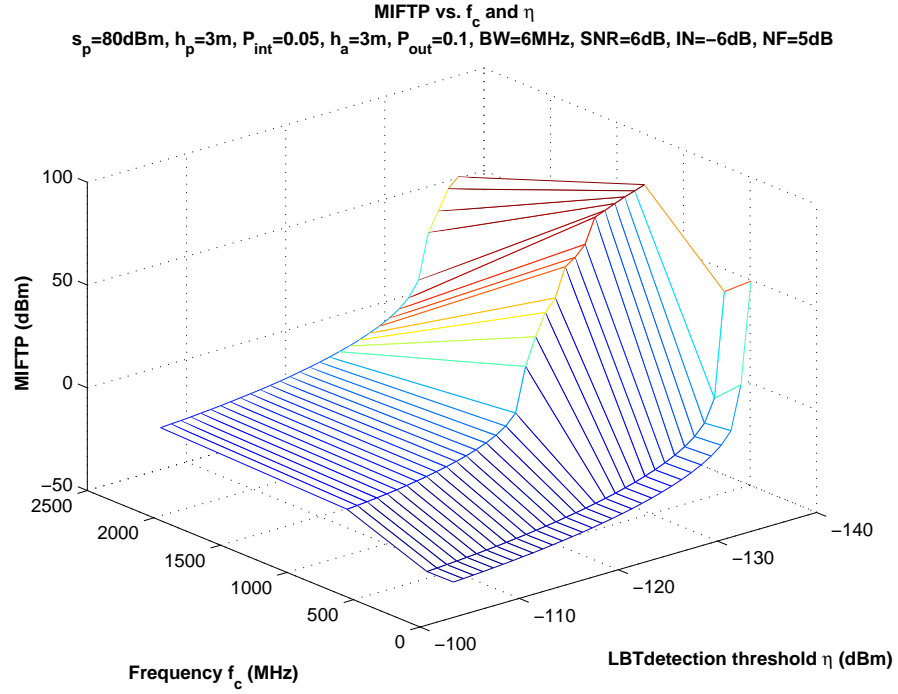


Fig. 11. MIFTP vs. carrier frequency and detection threshold.

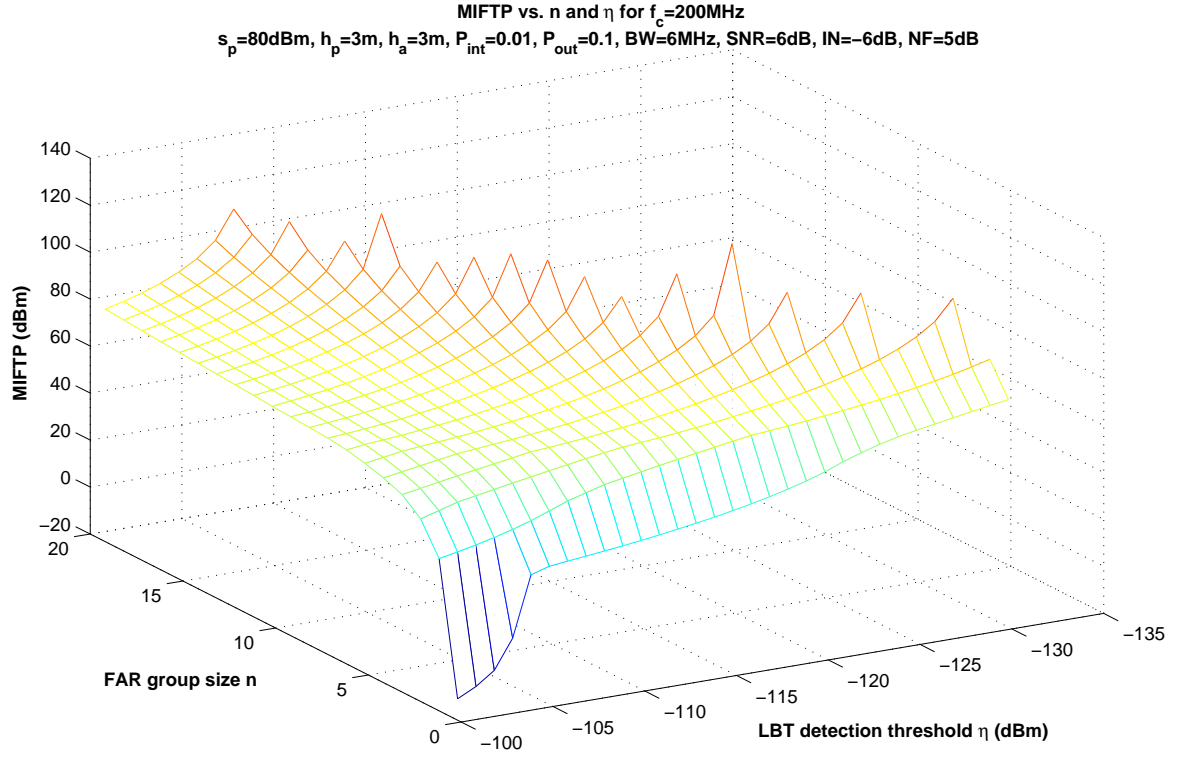


Fig. 12. MIFTP vs. detection threshold and FAR group size for collaborative sensing at $f_c = 200$ MHz.

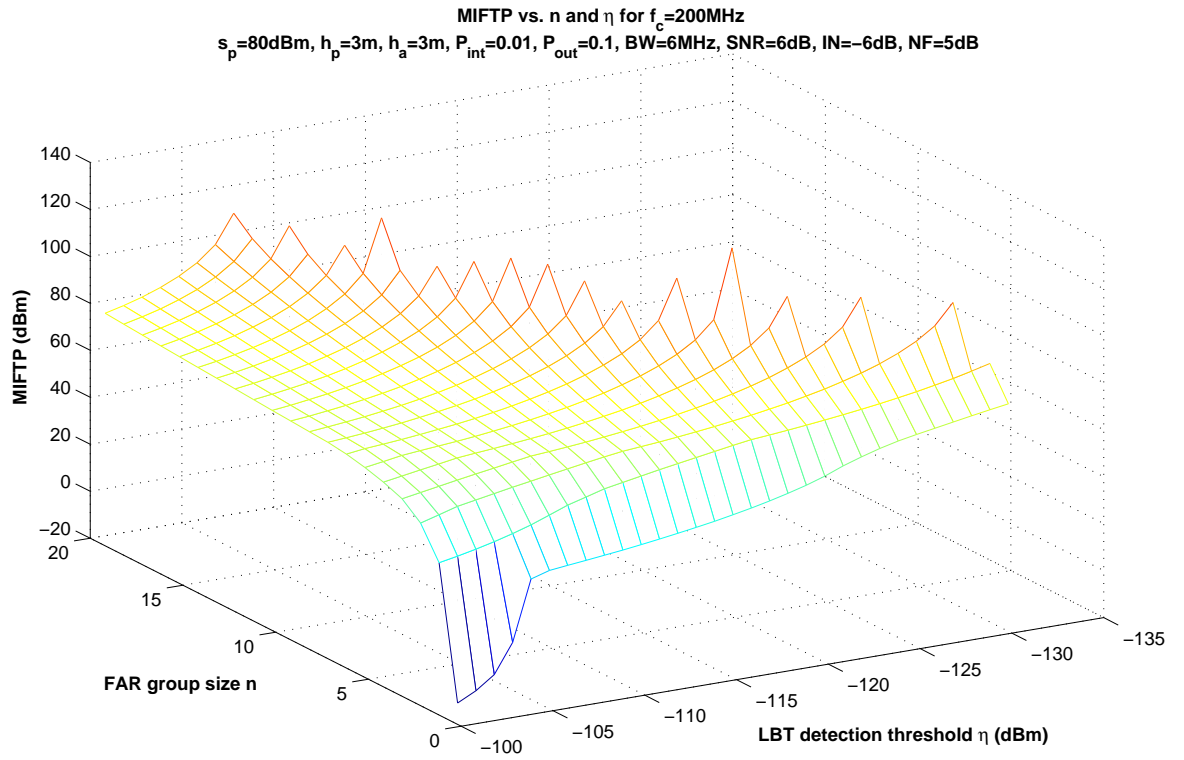


Fig. 13. MIFTP vs. detection threshold and FAR group size for collaborative sensing at $f_c = 2$ GHz

F. Collaborative LBT

Figs. 12 and 13 show MIFTP surfaces for collaborative LBT under homogeneous scenarios for carrier frequencies $f_c = 200$ MHz and $f_c = 2$ GHz, respectively. We see that the MIFTP increases with the number of FAR nodes in the group.

VII. CONCLUSION

We developed a framework to evaluate the performance of the basic Listen-Before-Talk (LBT) scheme and an extension of LBT called collaborative LBT that allows a group of FAR radios to collaborate. We introduced several important performance metrics including detection distance, interference distance, and maximum interference-free transmit power. These metrics can provide the basis for evaluating any spectrum access method. We derived expressions to evaluate these metrics with respect to the individual and collaborative LBT schemes and presented numerical results illustrating the relationships among them.

The numerical results show that the simple LBT can be used to harvest unused spectrum without causing harmful interference to existing users. The collaborative LBT scheme provides significantly higher spectrum capacity gains than individual LBT. The poorer performance of individual LBT is due to the fact that the nodes act without any knowledge about the location of the primary transmitter and the victim nodes. The collaborative LBT scheme provides additional information about the location of the primary implicitly through the use of alert messages. Spectrum sharing schemes employing more sophisticated collaborative behaviors should be able to harvest substantially more spectrum. In ongoing work, we are applying the analysis techniques developed in this paper to evaluate the performance of spectrum access with more complex group behaviors. The formulas derived in this paper for the performance metrics were based on the EPM-73 propagation model, which has a relatively simple closed form. In future work, we plan to evaluate the performance of spectrum access using more sophisticated models such as the TIREM and Longley-Rice models, together with spectrum measurement data obtained through drive test experiments.

REFERENCES

- [1] M. McHenry, "Frequency agile spectrum access technologies," in *Proc. FCC Workshop on Cognitive Radio*, May 2003.
- [2] G. Staple and K. Werbach, "The end of spectrum scarcity," *IEEE Spectrum*, vol. 41, pp. 48–52, March 2004.
- [3] S. Haykin, "Cognitive Radio: Brain-Empowered Wireless Communications," *IEEE J. Selected Areas in Comm.*, vol. 23, Feb. 2005.
- [4] J. Mitola *et al.*, "Cognitive radio: Making software radios more personal," *IEEE Pers. Commun.*, vol. 6, pp. 13–18, Aug. 1999.
- [5] A. E. Leu, K. Steadman, M. McHenry, and J. Bates, "Ultra Sensitive TV Detector Measurements," in *Proc. IEEE Int. Symp. on New Frontiers in Dynamic Spectrum Access Networks (DySPAN)*, pp. 30–36, Nov. 2005.
- [6] M. McHenry, "The Probe Spectrum Access Method," in *Proc. IEEE Int. Symp. on New Frontiers in Dynamic Spectrum Access Networks (DySPAN)*, pp. 346–351, Nov. 2005.
- [7] T. K. Fong, P. S. Henry, K. K. Leung, X. Qiu, and N. K. Shankaranarayanan, "Radio Resource Allocation in Fixed Broadband Wireless Networks," *IEEE Trans. on Comm.*, vol. 46, June 1998.
- [8] D. Raychaudhuri and X. Jing, "A spectrum etiquette protocol for efficient coordination of radio devices in unlicensed bands," in *Proc. PIMRC*, (Beijing, China), 2003.
- [9] O. Popescu and C. Rose, "Waterfilling may not good neighbors make," in *Proc. IEEE Globecom*, (Dallas, TX), pp. 1766–1770, Nov. 2004.
- [10] M. N. Lustgarten and J. A. Madsen, "An Empirical Propagation Model (EPM-73)," *IEEE Trans. on Electromagnetic Compatibility*, vol. 19, August 1977.
- [11] A. G. Longley and P. L. Rice, "Prediction of tropospheric transmission loss over irregular terrain, a computer method - 1968," ESSA 79-ITSS 67, U.S. Dept. of Commerce, Office of Telecommunications, Boulder, CO, July 1968.
- [12] A. G. Longley, G. H. Hufford, R. Reasoner, and J. Montgomery, "A statistical propagation model for the improved interference prediction model," ESSA OT-TM 67, U.S. Dept. of Commerce, Office of Telecommunications, Boulder, CO, Dec. 1971.
- [13] M. Weissburger *et al.*, "Radio Wave Propagation: A Handbook of Practical Techniques for Computing Basic Transmission Loss and Field Strength," Tech. Rep. AD-A122090, U.S. Dept. of Defense Electromagnetic Compatibility Analysis Center, Sept. 1982.